Heterogeneous Structures

Deutsche Ausgabe: DOI: 10.1002/ange.201607455
Internationale Ausgabe: DOI: 10.1002/anie.201607455

Fabrication of Hollow Materials by Fast Pyrolysis of Cellulose Composite Fibers with Heterogeneous Structures

*Yue Dong, Baoquan Jia, Feiya Fu, Heyou Zhang, Lina Zhang, and Jinping Zhou**

Abstract: *A facile method for the fabrication of inorganic hollow materials from cuprammonium cellulose composite filaments based on fast pyrolysis has been developed. Unlike Ostwald ripening, approaches based on the Kirkendall effect, and other template methods, this process yielded hollow materials within 100 s. The heterogeneous structure of the cellulose composite fibers and the gradient distribution of the metal oxides are the main reasons for the formation of the hollow structure. The diameter, wall thickness, and length of the hollow microfibers could be conveniently controlled. With their perfect morphology, these hollow structural materials have great potential for use in various fields.*

Hollow materials, as integrative structures with defined interior cavities, multifunctionalized shells, and tailored properties, have attracted considerable attention. Proper holes will endow the materials with large surface areas, closed cavities, and considerable inner volume to adapt to volume changes during electronic and catalytic processes, to protect cargo during delivery, or to form channels enabling the free movement of substances within the material. Owing to these advantages, many hollow materials have replaced their solid counterparts, and they have been applied in catalysis, drug delivery, lithium-ion batteries, and microchemical reactors.[1] Both template[2] and non-template[3] approaches have been explored to prepare hollow structural materials. Although significant progress has been made based on non-template methods, the design and synthesis of well-shaped hollow structural materials is mainly based on template methods. Complex hollow metal particles, cubes, and nanowires have usually been obtained by methods such as etching,[4] by making use of the Kirkendall effect,[5] and Ostwald ripening.[6] Coaxial spinning[7] and electrospinning[8] are often used for fabricating polymer-based fiber-like hollow materials. These methods are all efficient approaches but also suffer from various shortcomings, such as expensive precursors, low yields, time-consuming processes, or the need for special equipment. Therefore, it is still challenging to fabricate hollow materials in a self-templating, fast process from cheap precursors with high productivity and easy controllability.

Compared to the approaches known for the synthesis of hollow particles, methods for the fabrication of fiber-like hollow materials are limited and always involve the sintering of hollow or core–shell precursors.[9] Hollow fibers are free on their length, and both tube and annulus can be get from them. The multifunctional walls inside such hollow fibers can play various roles and act as catalysts or electrodes, for example. Furthermore, unlike hollow particles, hollow fibers are not hermetically closed but open, which extends their application in dynamic microreactors, consistent long-term delivery, and microfluidic chips.

Herein, we describe a new approach for the fabrication of complex inorganic hollow fibers through fast pyrolysis. Fast pyrolysis is a common method to obtain gases from polymers.[10] Metallic compounds often act as catalysts to increase the gas yield and reduce the amount of charcoal formed.[11] However, the residues obtained after pyrolysis have hardly been studied.[12] When a gradient distribution of catalyst was applied to the polymers, a gradient pyrolysis activity could be achieved within the matrix. Herein, we chose cuprammonium cellulose as the precursor. Cuprammonium solutions, which directly dissolve cellulose, have been used to obtain copper-based materials such as copper–cellulose nanocomposite films and helical fibers.[13] Moreover, it has been reported that the copper in the coagulated fibers decreases the crystallinity and the degree of fibril orientation in the regenerated cellulose (RC) fibers, which leads to low thermal stability during pyrolysis.[14] When cuprammonium cellulose filaments were subjected to fast pyrolysis in air or argon atmosphere, CuO and Cu@C hollow microfibers were obtained, respectively. The hollow structures were formed within 100 s, which is much quicker than by any other method. The as-obtained microfibers had two-level structures including several micrometer-wide circular channels and CuO or Cu nanoparticles (NPs) on the walls. The proposed strategy is also applicable to the synthesis of other metallic hollow fibers, and thus constitutes a facile, universal, productive, and environmentally friendly method for the preparation of hollow structural materials.

Dark brown CuO@RC composite filaments with diameters of 40–50 μm were obtained by wet spinning of a cuprammonium solution and drying in air under ambient conditions (see the Supporting Information, Figure S1). Figure 1 a shows a SEM image of the CuO@RC fibers. The composite fibers exhibit a dense and round cross-section. The surface of the fiber was comparatively rough because some CuO NPs were trapped on it. A TEM image highlights the transverse internal structure of the fibers (Figure 1 b). A hierarchical structure spontaneously formed among the CuO particles and the cellulose matrix. There is an approximately 3 μm thick ribbon

---

[*] Dr. Y. Dong, Dr. B. Jia, Dr. F. Fu, Dr. H. Zhang, Prof. L. Zhang, Prof. Dr. J. Zhou
Department of Chemistry and Key Laboratory of Biomedical Polymers of Ministry of Education
Wuhan University, Wuhan 430072 (China)
E-mail: zhoujp325@whu.edu.cn

Supporting information for this article can be found under: http://dx.doi.org/10.1002/anie.201607455.

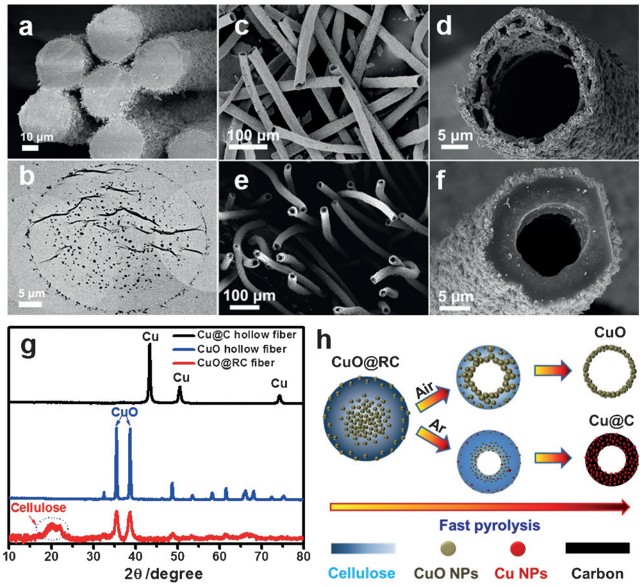

Figure 1. a) SEM and b) TEM images of the CuO@RC filaments. SEM images of c, d) CuO and of e, f) Cu@C hollow fibers. g) XRD patterns of CuO@RC fibers, CuO, and Cu@C hollow fibers. h) The formation of CuO and Cu@C hollow fibers by fast pyrolysis of CuO@RC filaments. The CuO and Cu@C hollow fibers were obtained by pyrolyzing the CuO@RC filaments at 600 °C for 1 h in air or argon atmosphere, respectively.

of cellulose, which contains barely any CuO NPs. The CuO particles in the fiber present a gradient distribution (Figure S2). Owing to this distributional difference, the fibers undergo both catalyzed and non-catalyzed pyrolysis at the same time, giving hollow structures. Figure S3 shows the thermogravimetric (TG) curves of CuO@RC composite fibers in air and argon atmosphere. The mass loss of the fibers in air atmosphere proceeded in four stages, and thermal degradation of cellulose was mainly observed at 280–340 °C. The CuO content in the composite fibers was determined to be about 30 wt %. The mass loss of the composite fibers in argon atmosphere proceeded in three stages. A major mass loss occurred in the temperature range of 300–400 °C, which was attributed to the thermal decomposition of cellulose and the reduction of the CuO particles.

When the CuO@RC filaments were pyrolyzed at 600 °C in air or argon atmosphere for 1 h, hollow CuO and Cu@C microfibers were obtained, respectively. The SEM images of the as-obtained fibers are shown in Figure 1 c–f. All of the fibers adopted a consummate and uniform hollow structure. The outer diameter and wall thickness of the CuO hollow fibers were about 20 and 2 μm, respectively. The Cu@C hollow fibers featured a solid shell with a finely grained structure, and the diameters of the whole fiber and the hollow channel were about 25 and 12 μm, respectively. Figure 1 g shows the XRD patterns of the CuO@RC fibers before and after thermal decomposition. The air-dried fibers were composed of CuO NPs (JCPDS No. 48-1548) and cellulose II. During pyrolysis in air, the cellulose was completely burned until only CuO remained. However, serious aggregation of CuO NPs occurred according to the decreasing peak widths in the XRD pattern. When pyrolyzed in argon atmosphere, Cu NPs (JCPDS No. 04-0836) were obtained through reduction of CuO by the cellulose matrix. The amount of Cu NPs in the Cu@C hollow fibers was determined to be 72 wt %.

To study the formation of the hollow structure, SEM, TEM, and XRD were used to characterize the morphology and structure of the fibers during pyrolysis. Figure S4 shows SEM images of CuO@RC fibers pyrolyzed at different temperatures for 1 h. When the pyrolysis temperature was 325 °C, a primitive hollow structure was formed in air atmosphere. The hollow structure became increasingly clearer with an increase in temperature (Figure S4 c, d). Under argon atmosphere, a primitive hollow structure was not observed until the pyrolysis temperature reached 350 °C. When the pyrolysis temperature was increased to 400 °C, the hollow channels had diameters of about 5 μm. With a further increase in pyrolysis temperature (Figure S5), the diameters of the hollow channels increased from 10 μm at 500 °C to 15 μm at 700 °C and 17 μm at 800 °C. By changing the pyrolysis temperature, we can thus adjust the hollow structure for different applications. As shown in Figure 1 h, we assume that hollow structures are first formed in the centers of the fibers in both atmospheres, which is accompanied by the migration and aggregation of CuO NPs. The pyrolysis process required a very fast heating rate. When a slow heating rate, such as 5 °C min^{-1} in air or 15 °C min^{-1} in argon, was applied, hollow structures were not observed (Figure S6).

Compared with the traditional template method,[15] the CuO NPs were distributed within the cellulose matrix instead of forming core–shell structures with RC fibers. SEM images of fibers pyrolyzed in air for 20 s are shown in Figure 2 a_1–a_4. Although most of the fibers have a hollow structure as shown in Figure 1 c and d, a series of interesting morphological changes were observed as a result of the heating. Specific heat cracks and decomposition were first observed at the center of the fiber. The hollow structure gradually developed in the crack area upon prolonged pyrolysis. We suggest that with the aid of oxygen, the formation of the hollow structure was very quick. When the material was subjected to pyrolysis for 40 s, all of the obtained fibers formed a hollow structure (Figure S7). When a fast pyrolysis was run in argon, porous structures with multiple pinholes started to emerge at the centers of the fibers after the initial 20 s (Figure 2 b_1). As the pyrolysis was continued, the pinholes expanded and connected with the other surrounding pinholes to form channels (Figure 2 b_2). These channels expanded and connected with the newly formed holes, finally turning into a single circular hollow structure (Figure 2 b_3 and b_4). Meanwhile, the shells of the fibers remained solid during the entire process.

While the TEM images in Figure 2 c_1–c_4 show the same morphologic changes as the SEM images, they also indicated that pinhole structures were only formed where the CuO NPs were located, suggesting that the CuO NPs exert a specific catalytic activity during the pyrolysis of cellulose. As the matrix at the center is reduced, the voids surrounding the CuO NPs facilitate their migration to the edge at high temperature, and they are finally reduced in argon. TEM images of fibers pyrolyzed in argon atmosphere at 700 °C for 80 s are displayed in Figure 2 d_1 and d_2. The diameter of the cross-section of the fiber barely changed, and the blank (non-

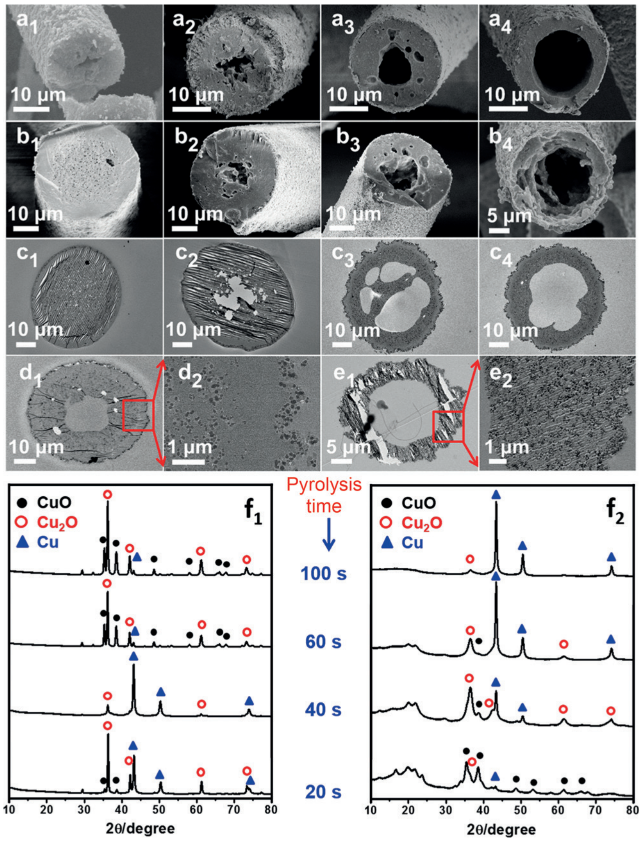

Figure 2. a$_1$–a$_4$) SEM images of CuO@RC fibers pyrolyzed in air at 600 °C for 20 s. b) SEM images of CuO@RC fibers pyrolyzed under argon atmosphere at 600 °C for b$_1$) 20, b$_2$) 40, b$_3$) 60, and b$_4$) 100 s. c–e) TEM images of CuO@RC fibers pyrolyzed under argon atmosphere at 600 °C for c$_1$) 20, c$_2$) 40, c$_3$) 60, and c$_4$) 100 s and at 700 °C for d$_1$, d$_2$) 80 s and e$_1$, e$_2$) 1 h. f) XRD patterns of CuO@RC fibers pyrolyzed f$_1$) in air and f$_2$) under argon atmosphere at 600 °C for different periods of time.

particle) zone (about 3 µm) could be clearly observed after the hollow structure had been formed. We suggest that the formation of the hollow structures differs from that obtained by Ostwald ripening or by making use of the Kirkendall effect, which rely on solid dissolution and growth or a solid-phase reaction. Our method is based on the specific thermal decomposition of the cellulose matrix and migration of the CuO particles. After carbonization at 700 °C for 1 h, the shell of the hollow fiber became a homogeneous mixture of Cu NPs and carbon (Figure 2 e$_1$, e$_2$). Our results show that the thermal decomposition occurred outwards from the center of the fiber, even though the heat was actually transferred from the outside to the center. Interestingly, the filaments obtained after combustion with a flame in air also exhibited a hollow structure (Figure S8). Therefore, CuO hollow fibers can be prepared on large scale through this facile and fast combustion method.

Figure 2 f$_1$ shows the XRD patterns of CuO@RC fibers pyrolyzed in air for different periods of time. The cellulose matrix quickly burned; no visible peaks representing cellulose II could be observed after pyrolysis for 20 s. The copper compounds underwent a series of constituent changes: In the first 20 s, most of the CuO NPs were reduced to form Cu_2O (JCPDS No. 05-0667) and Cu (JCPDS No. 04-0836). When pyrolyzed for 40 s, no peaks corresponding to CuO could be observed. Instead, plenty of Cu and a small amount of Cu_2O were observed as the decomposition of cellulose produced some reducing gas. After extended pyrolysis, CuO was again observed along with an increase in the amount of Cu_2O and a decrease in Cu. After pyrolysis for 1 h, only CuO remained (Figure 1 g). Figure 2 f$_2$ shows XRD patterns of CuO@RC fibers pyrolyzed in argon atmosphere for different periods of time. The diffraction peaks corresponding to cellulose II only disappeared after 60 s, when Cu_2O was observed as the primary product. The CuO had been completely transformed into Cu_2O and Cu after 100 s. After pyrolysis in argon atmosphere for 1 h, the CuO had been fully reduced, and only Cu was present (Figure 1 g). Furthermore, a pyrolysis gas chromatography mass spectrometry (Py-GC-MS) analysis was also used to trace the products during the fast pyrolysis (Figure S9). When CuO was introduced, the total yield of the main gaseous product increased. This finding indicates that the presence of CuO increases the conversion of cellulose into tar during pyrolysis, which was also beneficial for the formation of the hollow structures.

The formation mechanism suggested in Figure 1 h is in full agreement with these results although it is rather different from those proposed for conventional methods. In this work, the starting material is a heterogeneous CuO@RC solid fiber. It has been reported that the formation of copper chelates might affect the hydroxy groups in the C2 and C3 positions and inhibit the crystallization of cellulose.[14,16] The cellulose matrices of the fibers consisted of an outer, highly crystalline layer and an inner, amorphous section. Cellulose with a higher degree of crystallinity is known to benefit from enhanced thermal stability, that is, a higher decomposition temperature. During the pyrolysis, the CuO NPs catalyze the decomposition of the surrounding cellulose to produce mainly volatile compounds, leading to the formation of voids. As the centers of the fibers contain most of the CuO NPs, the voids emerged in the centers of the fibers and finally formed a single hole. The produced voids could also enable the migration of CuO NPs. When the CuO NPs finally migrated to the edge of the fiber, the cellulose on the edge had already undergone pyrolysis in a non-catalytic process. The remaining residues finally formed hollow CuO and Cu@C fibers in air and argon atmosphere, respectively.

The thermal decomposition of cellulose can be catalyzed by many metallic compounds to improve the yield of the volatile products.[17] Based on our method, other inorganic hollow materials were also fabricated (Figure 3). First, RC/Fe_2O_3, RC/$Cu(OH)_2$, RC/$MnO(OH)_2$, and RC/$NiCO_3$ composite fibers were prepared by in situ synthesis. When these composite fibers were sintered in air in a fast process, Fe_2O_3 (JCPDS No. 33-0664), CuO (JCPDS No. 48-1548), Mn_2O_3 (JCPDS No. 41-1442), and NiO (JCPDS No. 47-1049) hollow fibers were obtained. Similarly, Fe_3O_4@C (JCPDS No. 79-0629), Cu@C (JCPDS No. 04-0836), MnO@C (JCPDS No. 07-0230), and Ni@C (JCPDS No. 04-0850) hollow fibers were obtained after fast pyrolysis in argon atmosphere. Apart from cuprammonium cellulose as a one-pot mixture of metal and polymer, other metallic cellulose composite fibers can also

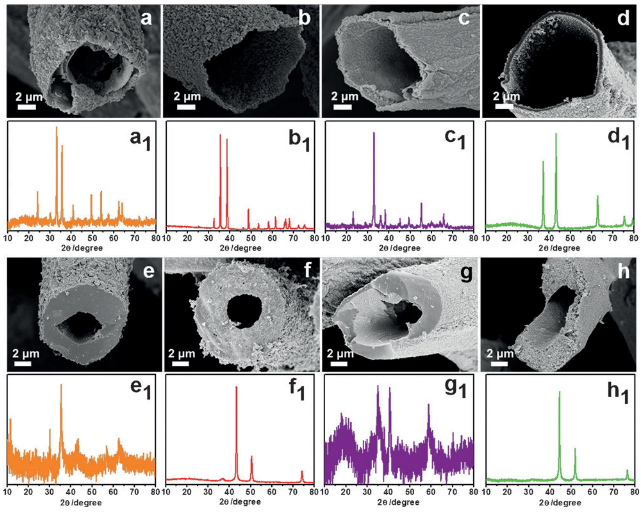

Figure 3. SEM images and XRD patterns of a, a$_1$) Fe_2O_3, b, b$_1$) CuO, c, c$_1$) Mn_2O_3, and d, d$_1$) NiO hollow fibers prepared by pyrolysis in air for 1 h. SEM images and XRD patterns of e, e$_1$) Fe_3O_4@C, f, f$_1$) Cu@C, g, g$_1$) MnO@C, and h, h$_1$) Ni@C hollow fibers obtained by pyrolysis in argon atmosphere for 1 h.

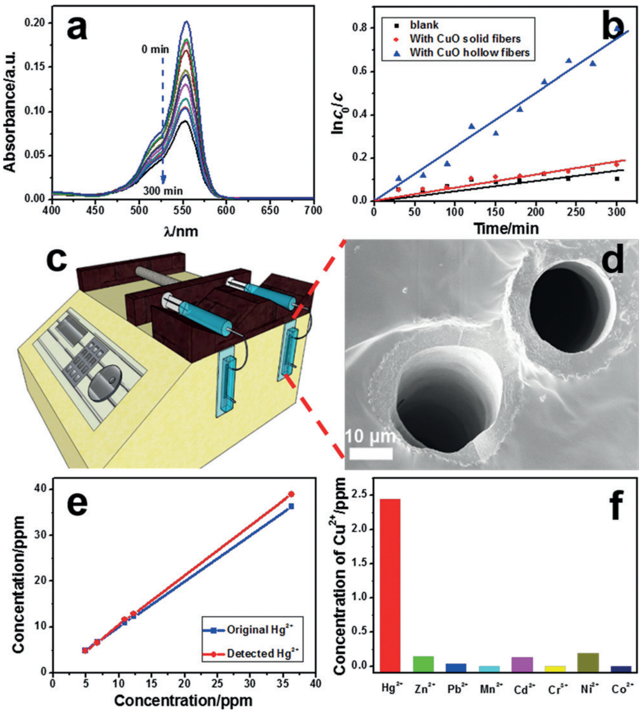

Figure 4. Degradation of RhB with H_2O_2 in the presence of CuO hollow fibers. a) UV/Vis spectra. b) Apparent reaction kinetic curves (c_0 = initial RhB concentration, c = current RhB concentration). Detection of Hg^{2+} with microfluidic chips of Cu@C hollow fibers. c) The device for injecting analytes. d) SEM image of Cu@C hollow fibers embedded in PDMS. e) Detection of Hg^{2+} at different concentrations. f) Specific detection of Hg^{2+} retained by Cu@C hollow fibers.

yield hollow structures through fast pyrolysis, indicating that the combination of RC fibers and metallic derivatives is a perfect precursor for the synthesis of inorganic hollow materials. This widely applicable approach should extend the use of hollow fibers in various fields.

As a p-type semiconductor, CuO is a versatile metal oxide with potential in various applications, such as catalysis.[18] The catalytic activity of the CuO fibers was tested in the oxidative degradation of rhodamine B (RhB) with H_2O_2 at 25 °C (Figure 4 a, b). After 5 h, RhB had been degraded with the aid of the CuO hollow fibers (Figure 4 a). The CuO hollow fibers displayed good catalytic activity although obvious aggregation had occurred during the sintering process. The degradation of RhB was slow in the absence of CuO hollow fibers. Meanwhile, CuO solid fibers were significantly less catalytically active, indicating that the hollow structure played an important role in catalyzing the degradation of RhB.

The micrometer-sized cylindrical holes and dense tube walls of the Cu@C hollow fibers are ideal for their direct application in microfluidic chips. A simple syringe pump was chosen to inject analytes at different concentrations through the prepared chip (Figure 4 c). The hollow fibers maintained their expedite holes after embedment into polydimethylsiloxane (PDMS; Figure 4 d). Moreover, the PDMS combined tightly with the walls of the Cu@C hollow fibers so that the liquid analyte had to pass through the hollow channels. As they naturally contain Cu NPs, we used a general replacement reaction to test their function as a chip channel [Eq. (1) and (2)].[19]

$$\mathrm{Cu} + \mathrm{Hg}^{2+} \rightarrow \mathrm{Cu}^{2+} + \mathrm{Hg} \tag{1}$$

$$x\,\mathrm{Cu} + y\,\mathrm{Hg} \rightarrow \mathrm{Cu}_x\mathrm{Hg}_y \tag{2}$$

As shown in Figure 4 e, for lower concentrations (< 40 ppm), retention of the targeted Hg^{2+} ions was quantitative with respect to the amount in the original solution. Figure 4 f illustrates the selective adsorption and reaction properties of the hollow fibers by giving the Cu^{2+} concentration of the effluents from metal ion solutions with the same concentration. Except for Hg^{2+}, which gave a concentration equimolar to that of Cu^{2+}, the other effluents gave low Cu^{2+} concentrations close to zero. This indicated that the Cu@C hollow fibers could act as specific functionalized microfluidic chip channels. Owing to their functionalized walls, the hollow fibers can adsorb and be used for the detection of Hg^{2+} without post-modification while avoiding the handling of toxic compounds during analysis.

In summary, a facile fast-pyrolysis method has been developed for the fabrication of inorganic hollow structural materials. The CuO@RC composite fibers consisted of low-crystalline cellulose and a high concentration of CuO NPs on the inside. This heterogeneous structure enabled the specific thermal decomposition of the cellulose matrix and migration of the CuO NPs from the center to the edges of the fibers during pyrolysis. Finally, CuO and Cu@C hollow microfibers with controllable sizes and morphologies were obtained in air and argon atmosphere, respectively. Aside from the copper-based hollow fibers, other metallic hollow structural materials were also prepared through this method. The proposed strategy to create hollow fibers could be easily scaled up and avoids the use of expensive starting materials and elaborate processes. Moreover, the obtained inorganic hollow materials could find applications in catalysis, microreactors, and microfluidics, for example.

Acknowledgements

This work was financially supported by the National Natural Science Foundation of China (51273151 and 51473128).

Keywords: cellulose · CuO nanoparticles · heterogeneous structures · hollow fibers · pyrolysis

How to cite: *Angew. Chem. Int. Ed.* **2016**, *55*, 13504–13508
Angew. Chem. **2016**, *128*, 13702–13706

---

[1] a) Y. Zhao, L. Jiang, *Adv. Mater.* **2009**, *21*, 3621–3638; b) X. Liu, X. Jin, P. X. Ma, *Nat. Mater.* **2011**, *10*, 398–406; c) Z. Zhang, Y. Chen, X. Xu, J. Zhang, G. Xiang, W. He, X. Wang, *Angew. Chem. Int. Ed.* **2014**, *53*, 429–433; *Angew. Chem.* **2014**, *126*, 439–443; d) E. G. Moschetta, S. Negretti, K. M. Chepiga, N. A. Brunelli, Y. Labreche, Y. Feng, F. Rezaei, R. P. Lively, W. J. Koros, H. M. L. Davies, C. W. Jones, *Angew. Chem. Int. Ed.* **2015**, *54*, 6470–6474; *Angew. Chem.* **2015**, *127*, 6570–6574; e) G. Zhang, X. W. Lou, *Angew. Chem. Int. Ed.* **2014**, *53*, 9041–9044; *Angew. Chem.* **2014**, *126*, 9187–9190.

[2] a) L. Yu, L. Zhang, H. Wu, X. W. Lou, *Angew. Chem. Int. Ed.* **2014**, *53*, 3711–3714; *Angew. Chem.* **2014**, *126*, 3785–3788; b) J. Liu, N. P. Wickramaratne, S. Z. Qiao, M. Jaroniec, *Nat. Mater.* **2015**, *14*, 763–774.

[3] a) X. B. Cao, L. Gu, L. J. Zhuge, W. J. Gao, W. C. Wang, S. F. Wu, *Adv. Funct. Mater.* **2006**, *16*, 896–902; b) H. Yu, J. Yu, S. Liu, S. Mann, *Chem. Mater.* **2007**, *19*, 4327–4334; c) A. Pan, H. B. Wu, L. Yu, X. W. Lou, *Angew. Chem. Int. Ed.* **2013**, *52*, 2226–2230; *Angew. Chem.* **2013**, *125*, 2282–2286.

[4] T. Jaumann, M. Herklotz, M. Klose, K. Pinkert, S. Oswald, J. Eckert, L. Giebeler, *Chem. Mater.* **2015**, *27*, 37–43.

[5] a) H. J. Fan, M. Knez, R. Scholz, K. Nielsch, E. Pippel, D. Hesse, M. Zacharias, U. Gösele, *Nat. Mater.* **2006**, *5*, 627–631; b) H. J. Fan, M. Knez, R. Scholz, D. Hesse, K. Nielsch, M. Zacharias, U. Gösele, *Nano Lett.* **2007**, *7*, 993–997; c) G. Song, C. Liang, X. Yi, Q. Zhao, L. Cheng, K. Yang, Z. Liu, *Adv. Mater.* **2016**, *28*, 2716–2723.

[6] a) X. Sun, J. Liu, Y. Li, *Chem. Mater.* **2006**, *18*, 3486–3494; b) C. C. Yec, H. C. Zeng, *J. Mater. Chem. A* **2014**, *2*, 4843–4851; c) L. Cao, D. Chen, R. A. Caruso, *Angew. Chem. Int. Ed.* **2013**, *52*, 10986–10991; *Angew. Chem.* **2013**, *125*, 11192–11197.

[7] Y. Zhao, C. Jiang, C. Hu, Z. Dong, J. Xue, Y. Meng, N. Zheng, P. Chen, L. Qu, *ACS Nano* **2013**, *7*, 2406–2412.

[8] K. Müller, J. F. Quinn, A. P. R. Johnston, M. Becker, A. Greiner, F. Caruso, *Chem. Mater.* **2006**, *18*, 2397–2403.

[9] a) X. Huang, J. Zhang, Z. Liu, T. Sang, B. Song, H. Zhu, C. Wong, *J. Alloys Compd.* **2015**, *648*, 1072–1075; b) H. Guo, R. Mao, X. Yang, S. Wang, J. Chen, *J. Power Sources* **2012**, *219*, 280–284; c) X. Zhang, D. K. Wang, D. R. S. Lopez, J. C. D. da Costa, *Chem. Eng. J.* **2014**, *236*, 314–322.

[10] a) J. Huo, L. Wang, E. Irran, H. Yu, J. Gao, D. Fan, B. Li, J. Wang, W. Ding, A. Amin, C. Li, L. Ma, *Angew. Chem. Int. Ed.* **2010**, *49*, 9237–9241; *Angew. Chem.* **2010**, *122*, 9423–9427; b) R. J. White, K. Tauer, M. Antonietti, M.-M. Titirici, *J. Am. Chem. Soc.* **2010**, *132*, 17360–17363; c) R. Liu, S. M. Mahurin, C. Li, R. R. Unocic, J. C. Idrobo, H. Gao, S. J. Pennycook, S. Dai, *Angew. Chem. Int. Ed.* **2011**, *50*, 6799–6802; *Angew. Chem.* **2011**, *123*, 6931–6934; d) L. Li, C. Yuan, D. Zhou, A. E. Ribbe, K. R. Kittilstved, S. Thayumanavan, *Angew. Chem. Int. Ed.* **2015**, *54*, 12991–12995; *Angew. Chem.* **2015**, *127*, 13183–13187.

[11] D. Fabbri, C. Torri, V. Baravelli, *J. Anal. Appl. Pyrolysis* **2007**, *80*, 24–29.

[12] a) E. Ghadiri, N. Taghavinia, S. M. Zakeeruddin, M. Gratzel, J. E. Moser, *Nano Lett.* **2010**, *10*, 1632–1638; b) R. Mao, H. Guo, D. X. Tian, X. J. Yang, S. X. Wang, J. Chen, *J. Inorg. Mater.* **2013**, *28*, 1213–1217.

[13] a) B. Jia, Y. Mei, L. Cheng, J. Zhou, L. Zhang, *ACS Appl. Mater. Interfaces* **2012**, *4*, 2897–2902; b) B. Jia, Y. Dong, J. Zhou, L. Zhang, *J. Mater. Chem. C* **2014**, *2*, 524–529; c) B. Jia, L. Yu, F. Fu, L. Li, J. Zhou, L. Zhang, *RSC Adv.* **2014**, *4*, 9112–9117.

[14] H. Miyamoto, C. Yamane, M. Mori, K. Okajima, J. Sugiyama, *Text. Res. J.* **2009**, *79*, 694–701.

[15] a) J. Huang, N. Matsunaga, K. Shimanoe, N. Yamazoe, T. Kunitake, *Chem. Mater.* **2005**, *17*, 3513–3518; b) J. Huang, K. Toyoki, *J. Mater. Chem.* **2006**, *16*, 4257–4264; c) S. Liu, L. Zhang, J. Zhou, J. Xiang, J. Sun, J. Guan, *Chem. Mater.* **2008**, *20*, 3623–3628; d) N. Kang, J. H. Park, M. Jin, N. Park, S. M. Lee, H. J. Kim, J. M. Kim, S. U. Son, *J. Am. Chem. Soc.* **2013**, *135*, 19115–19117.

[16] I. Miyamoto, M. Inamoto, T. Matsui, M. Saito, K. Okajima, *Polym. J.* **1995**, *27*, 1113–1122.

[17] a) G. Dobele, G. Rossinskaja, T. Dizhbite, G. Telysheva, D. Meier, O. Faix, *J. Anal. Appl. Pyrolysis* **2005**, *74*, 401–405; b) M. Zhao, N. H. Florin, A. T. Harris, *Appl. Catal. B* **2009**, *92*, 185–193.

[18] a) H. Li, J. Liao, T. Zeng, *Catal. Commun.* **2014**, *46*, 169–173; b) H. Shi, Y. Zhao, N. Li, K. Wang, X. Hua, M. Chen, F. Teng, *Catal. Commun.* **2014**, *47*, 7–12.

[19] a) W. Ren, C. Zhu, E. Wang, *Nanoscale* **2012**, *4*, 5902–5909; b) L. Manganiello, A. Ríos, M. Valcárcel, *Anal. Chem.* **2002**, *74*, 921–925; c) L. Deng, X. Ouyang, J. Jin, C. Ma, Y. Jiang, J. Zheng, J. Li, Y. Li, W. Tan, R. Yang, *Anal. Chem.* **2013**, *85*, 8594–8600; d) V. Chakrapani, K. B. Ayaz Ahmed, V. Kumar, V. Ganapathy, S. P. Anthony, V. Anbazhagan, *RSC Adv.* **2014**, *4*, 33215–33221.

Received: August 1, 2016
Revised: September 7, 2016